

**Synthesis, Characterization, and DNA-Binding Properties of the Chiral Ruthenium(II) Complexes  $\Delta$ - and  $\Lambda$ -[Ru(bpy)<sub>2</sub>(dmppd)]<sup>2+</sup> (dmppd = 10,12-Dimethylpteridino[6,7-*f*][1,10]phenanthroline-11,13(10*H*,12*H*)-dione; bpy = 2,2'-Bipyridine)**

by Feng Gao<sup>a)</sup>), Hui Chao<sup>\*a)</sup>), Feng Zhou<sup>a)</sup>, Lian-Cai Xu<sup>a)</sup>, Kang-Cheng Zheng<sup>a)</sup>,  
and Liang-Nian Ji<sup>\*a)</sup>)

<sup>a)</sup> Key Laboratory of Bioinorganic and Synthetic Chemistry of the Ministry of Education, School of Chemistry and Chemical Engineering, Sun Yat-Sen University, Guangzhou 510275, P. R. China  
(fax: 86-20-84035497; e-mail: ceschh@mail.sysu.edu.cn)

<sup>b)</sup> Department of Chemistry, Tongji University, Shanghai 200092, P. R. China

<sup>c)</sup> State Key Laboratory of Coordination Chemistry, Nanjing University, Nanjing 210093, P. R. China

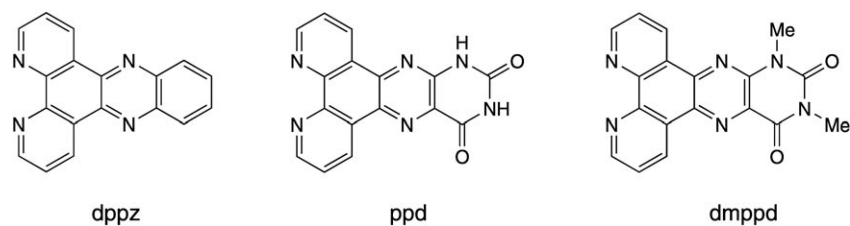
---

Two novel chiral ruthenium(II) complexes,  $\Delta$ -[Ru(bpy)<sub>2</sub>(dmppd)]<sup>2+</sup> and  $\Lambda$ -[Ru(bpy)<sub>2</sub>(dmppd)]<sup>2+</sup> (dmppd = 10,12-dimethylpteridino[6,7-*f*][1,10]phenanthroline-11,13(10*H*,12*H*)-dione, bpy = 2,2'-bipyridine), were synthesized and characterized by elemental analysis, <sup>1</sup>H-NMR and ES-MS. The DNA-binding behaviors of both complexes were studied by UV/VIS absorption titration, competitive binding experiments, viscosity measurements, thermal DNA denaturation, and circular-dichroism spectra. The results indicate that both chiral complexes bind to calf-thymus DNA in an intercalative mode, and the  $\Delta$  enantiomer shows larger DNA affinity than the  $\Lambda$  enantiomer does. Theoretical-calculation studies for the DNA-binding behaviors of these complexes were carried out by the density-functional-theory method. The mechanism involved in the regulating and controlling of the DNA-binding abilities of the complexes was further explored by the comparative studies of [Ru(bpy)<sub>2</sub>(dmppd)]<sup>2+</sup> and of its parent complex [Ru(bpy)<sub>2</sub>(ppd)]<sup>2+</sup> (ppd = pteridino[6,7-*f*][1,10]phenanthroline-11,13(10*H*,12*H*)-dione).

---

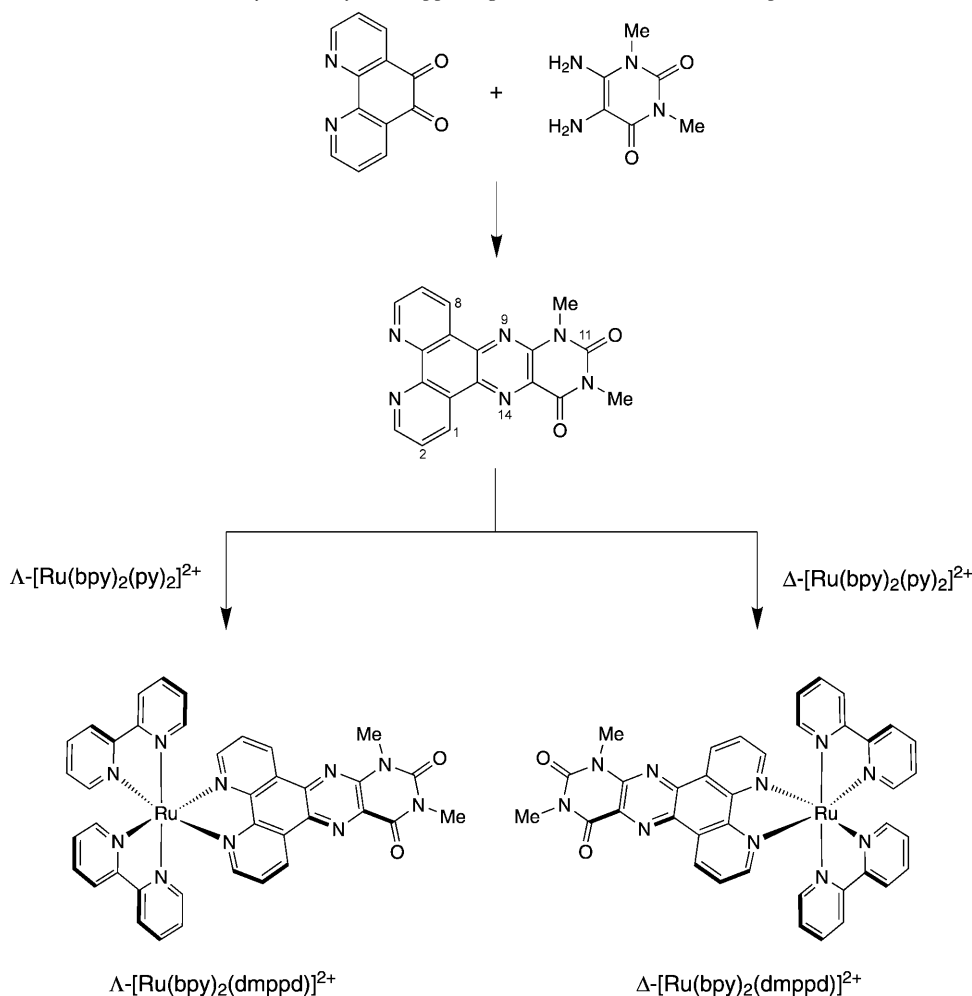
**1. Introduction.** – DNA-Binding studies of small molecules are very important in the development of DNA molecular probes and new therapeutic reagents [1–3]. In particular, (polypyridine)ruthenium(II) complexes, due to their easily constructed rigid chiral structures spanning all three spatial dimensions and rich photophysical properties, have received considerable attention [4–7]. The exact binding mode to DNA of the parent [Ru(phen)<sub>3</sub>]<sup>2+</sup> complex has been a controversial issue [8–10] (phen = 1,10-phenanthroline). However, modified, more extended ligands can be classical DNA intercalators, *e.g.*, the well-known dipyrido[3,2-*a*:2',3'-*c*]phenazine (dppz; see *Fig. 1*) whose complexes [Ru(bpy)<sub>2</sub>(dppz)]<sup>2+</sup> and [Ru(phen)<sub>2</sub>(dppz)]<sup>2+</sup> (bpy = bipyridine) have emerged as the most promising metal-based molecular probes of DNA and which possesses some interesting properties [11–13].

It is well established that the geometry of the complex binding to DNA is a very important factor in the study of the interactions of metallointercalators with nucleic acids. Thus modifying the ligands or changing substituents can create some interesting differences in the space filling and the electronic structures of (polypyridine)ruthenium(II) complexes, which will result in some important differences in the DNA-binding behaviors and spectral properties of the complexes, and thus will be helpful for a

Fig. 1. *Ligands*

better understanding of the binding mechanism of (polypyridine)ruthenium(II) complexes to DNA. Recently, we have designed and synthesized a novel Ru<sup>II</sup> complex  $[\text{Ru}(\text{bpy})_2(\text{ppd})]^{2+}$  (ppd = pteridino[6,7-*f*][1,10]phenanthroline-11,13(10*H*,12*H*)-dione; see Fig. 1) by replacing the terminal benzene ring of  $[\text{Ru}(\text{bpy})_2(\text{dppz})]^{2+}$  with a uracil moiety, a pyrimidine base of nucleic acids.  $[\text{Ru}(\text{bpy})_2(\text{ppd})]^{2+}$  has been found to intensively intercalate between the DNA base pairs and serves as a highly sensitive luminescent sensor for double-strand DNA [14]. To obtain more insight into the relation between the structure of such complexes and their DNA-binding abilities, two Me groups were now introduced into the structure of ppd, and a pair of chiral complexes  $\Delta$ - $[\text{Ru}(\text{bpy})_2(\text{dmppd})]^{2+}$  and  $\Lambda$ - $[\text{Ru}(\text{bpy})_2(\text{dmppd})]^{2+}$  (dmppd = 10,12-dimethylpteridino[6,7-*f*][1,10]phenanthroline-11,13(10*H*,12*H*)-dione; see Fig. 1) were synthesized. The DNA-binding behaviors of these new complexes were studied by UV/VIS absorption titration, competitive binding experiments with ethidium bromide (EB), viscosity measurements, thermal DNA denaturation, and circular dichroism (CD) spectra. All results suggested that both chiral complexes bind to DNA in an intercalative mode, the DNA-binding ability of the  $\Delta$  enantiomer being stronger than that of the  $\Lambda$  enantiomer. The fact that the intrinsic binding constants of both chiral complexes are smaller than that of their parent complex  $[\text{Ru}(\text{bpy})_2(\text{ppd})]^{2+}$  prompted us to envisage different mechanisms involved in the regulating and controlling of the DNA-binding abilities of complexes. Theoretical calculations with the density-functional-theory (DFT) method were carried out which furnished information about the molecular structures and molecular orbitals of the synthesized complexes, thus allowing to explain some of the experimental observations.

**2. Results and Discussion.** – 2.1. *Synthesis and Characterization.* As shown in the *Scheme*, the ligand dmppd was synthesized by the condensation of 1,10-phenanthroline-5,6-dione and 5,6-diamino-1,3-dimethyluracil (= 5,6-diamino-1,3-dimethylpyrimidine-2,4(1*H*,3*H*)-dione) [15]. The chiral precursors  $\Delta$ - $[\text{Ru}(\text{bpy})_2(\text{py})_2][O, O'-dibenzoyl-*D*-tartrate] · 12 H<sub>2</sub>O and  $\Lambda$ - $[\text{Ru}(\text{bpy})_2(\text{py})_2][O, O'-dibenzoyl-*L*-tartrate] · 12 H<sub>2</sub>O (py = pyridine) were synthesized according to [16]; only the crystalline samples were used to assure the enantiomer purity, and corresponding CD spectra were obtained. The target chiral ruthenium(II) complexes were then synthesized by treating the chiral precursors with dmppd, isolated as the perchlorate salts, and purified by column chromatography. The ES-MS show only isotope peaks corresponding to  $[M - 2 \text{ClO}_4^- - \text{H}]^+$  and  $[M - 2 \text{ClO}_4^-]^{2+}$ , and the measured molecular masses are consistent with the expected values.$$

Scheme. Synthesis of the dmppd Ligand and the Chiral Ru<sup>II</sup> Complexes

The complexes  $\Delta$ - and  $\Lambda$ -[Ru(bpy)<sub>2</sub>(dmppd)]<sup>2+</sup> give well-defined <sup>1</sup>H-NMR spectra, exhibiting only slight differences in the chemical shifts (see *Exper. Part*), which permit an unambiguous identification and assessment of their purity. The  $\delta$ (H) were assigned by comparison with those of similar complexes [17–23]. Due to the distinct shielding influences of the adjacent bpy and dmppd, the two halves of each bpy are not chemically and magnetically equivalent, leading to eight signals for the bpy protons, a set of four at higher field arising from the half of bpy near the dmppd and another set of four at lower field arising from the half of bpy near the other bpy, in accord with the greater shielding effect of dmppd than that of bpy. The small differences between the <sup>1</sup>H-NMR spectra of the two complexes is likely originating from the slight difference of the chemical environment of the two enantiomers, which is induced by the chi-

ral structure. Many other chiral (polypyridine)ruthenium(II) complexes have shown a similar behavior [24][25].

The CD spectra of  $\Delta$ - and  $\Lambda$ -[Ru(bpy)<sub>2</sub>(dmppd)]<sup>2+</sup> are rather similar to those of other chiral [Ru(bpy)<sub>2</sub>(L)]<sup>2+</sup> complexes, both in the MLCT (metal-to-ligand charge transfer) bands and the bands in the UV region. The enantiomer purity was determined by employing a reported method [26]. The analysis was calibrated by adding 5% of the  $\Delta$  enantiomer to the standard sample, establishing that the prepared  $\Lambda$  enantiomer contained less than 2% of  $\Delta$  enantiomer. Comparison of CD spectra (relative to absorption intensities) established the same optical purity (98%) for the  $\Delta$  enantiomer [27].

**2.2. Molecular Structures and Molecular Orbitals.** Molecular geometric structures and the energy and population of the frontier molecular orbitals (MOs) of ruthenium(II) complexes can strongly affect their DNA-binding behaviors. Therefore, an estimate of these characteristics of the synthesized complexes may be helpful to understand the following experimental results.

The molecular geometric structures of [Ru(bpy)<sub>2</sub>(dmppd)]<sup>2+</sup> and of its parent complex [Ru(bpy)<sub>2</sub>(ppd)]<sup>2+</sup> were obtained by full geometry optimizations with the DFT method at the B3LYP/LanL2DZ level. From the optimized structures of the complexes (Fig. 2), we can see that [Ru(bpy)<sub>2</sub>(dmppd)]<sup>2+</sup> still retains an excellent planarity, as [Ru(bpy)<sub>2</sub>(ppd)]<sup>2+</sup> does, and the  $\pi$ -conjugated aromatic area of dmppd is also similar to ppd. This observation implies that [Ru(bpy)<sub>2</sub>(dmppd)]<sup>2+</sup> may bind DNA with similar affinity as [Ru(bpy)<sub>2</sub>(ppd)]<sup>2+</sup>, which is higher than most of the other ruthenium(II) complexes [28]. On the other hand, the two bulky Me groups of [Ru(bpy)<sub>2</sub>(dmppd)]<sup>2+</sup> may sterically interfere on intercalation with DNA and lead to a decrease of the binding constant of the complex with DNA, as compared to [Ru(bpy)<sub>2</sub>(ppd)]<sup>2+</sup>.

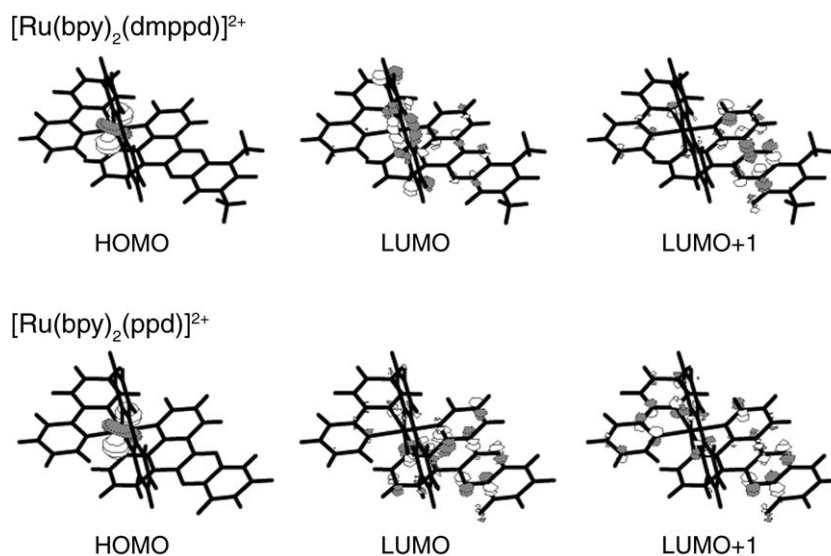


Fig. 2. Contour plots of some related frontier molecular orbitals of the complexes [Ru(bpy)<sub>2</sub>(dmppd)]<sup>2+</sup> and [Ru(bpy)<sub>2</sub>(ppd)]<sup>2+</sup>

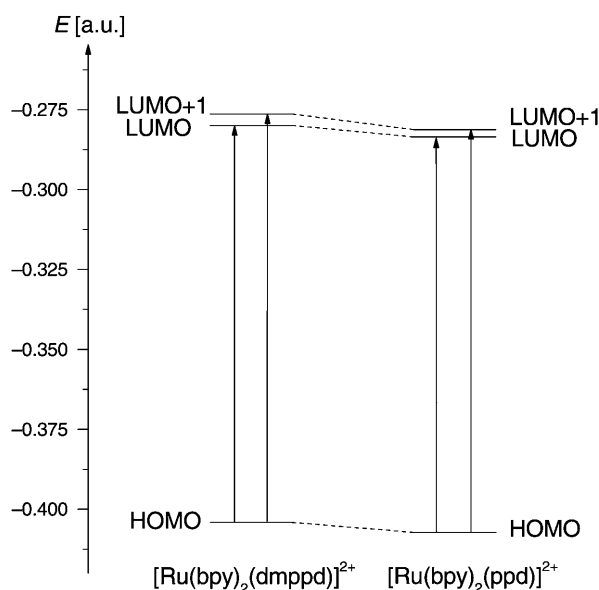


Fig. 3. Energy diagram of some frontier molecular orbitals and related 1 MLCT of the complexes  $[\text{Ru}(\text{bpy})_2(\text{dmppd})]^{2+}$  and  $[\text{Ru}(\text{bpy})_2(\text{ppd})]^{2+}$

From the energy diagrams of the frontier MOs of  $[\text{Ru}(\text{bpy})_2(\text{dmppd})]^{2+}$  and  $[\text{Ru}(\text{bpy})_2(\text{ppd})]^{2+}$  (Fig. 3), we can see that the energy of LUMO+1 is very close to that of LUMO, therefore, the MLCT may occur between both HOMO to LUMO and HOMO to LUMO + 1. The LUMO energy of  $[\text{Ru}(\text{bpy})_2(\text{ppd})]^{2+}$  is lower than that of  $[\text{Ru}(\text{bpy})_2(\text{dmppd})]^{2+}$ . For this reason, electron transfer from DNA is less favorable for  $[\text{Ru}(\text{bpy})_2(\text{dmppd})]^{2+}$  than for  $[\text{Ru}(\text{bpy})_2(\text{ppd})]^{2+}$ , and as a result, the DNA-binding ability of the former may be somewhat lower than that of the latter [29][30]. On the other hand, from the plots of the frontier MOs (Fig. 3), we can see that the HOMOs of both  $[\text{Ru}(\text{bpy})_2(\text{dmppd})]^{2+}$  and  $[\text{Ru}(\text{bpy})_2(\text{ppd})]^{2+}$  have mainly contributions from the central ruthenium(II) atom, while the LUMOs and LUMO + 1s of both complexes are mostly composed of the MOs of the ligands dmppd, ppd, and bpy. A majority of LUMO and LUMO + 1 of  $[\text{Ru}(\text{bpy})_2(\text{ppd})]^{2+}$  are distributed on ppd, while the LUMO and LUMO + 1 of  $[\text{Ru}(\text{bpy})_2(\text{dmppd})]^{2+}$  are less distributed on dmppd. Therefore, when the complexes intercalate into DNA base pairs, the LUMO and LUMO + 1 of  $[\text{Ru}(\text{bpy})_2(\text{ppd})]^{2+}$  are more prone to overlap with the HOMO of DNA than those of  $[\text{Ru}(\text{bpy})_2(\text{dmppd})]^{2+}$ .

Conclusively, the results of the theoretical calculations on the molecular geometric structures and the energy and population of the frontier MOs indicate that the methylation of ppd to dmppd may reduce the DNA-binding abilities of the ruthenium(II) complexes. Considering that the difference of the energy of the MOs is not very distinct, the steric effect of the Me groups is likely to have a greater influence.

2.3. DNA-Binding Studies. 2.3.1. UV/VIS Absorption Titrations. The UV/VIS absorption spectra of the complexes  $\Delta$ - and  $\Lambda$ - $[\text{Ru}(\text{bpy})_2(\text{dmppd})]^{2+}$  in the absence and presence of calf-thymus DNA (CT-DNA) at various DNA concentrations are

given in Fig. 4. The patterns and shapes of the spectra are similar to those of the structurally corresponding homoleptic complexes  $[\text{Ru}(\text{bpy})_2(\text{ppd})]^{2+}$  reported previously [14]. The absorption spectra of  $\Delta$ - and  $\Lambda$ - $[\text{Ru}(\text{bpy})_2(\text{dmppd})]^{2+}$  are characterized by distinct intense MLCT transitions in the VIS region, which are attributed to  $\text{Ru}(\text{d}\pi) \rightarrow \text{bpy}(\pi^*)$  and  $\text{Ru}(\text{d}\pi) \rightarrow \text{dmppd}(\pi^*)$  transitions. The bands below 300 nm are attributed to intraligand (IL)  $\pi\text{-}\pi^*$  transitions and those at 375 and 388 nm to the  $\pi\text{-}\pi^*$  transition of dmppd [15]. As the concentration of DNA is increased, the hypochromism in the MLCT band increases although no obvious red shift is observed. The hypochro-

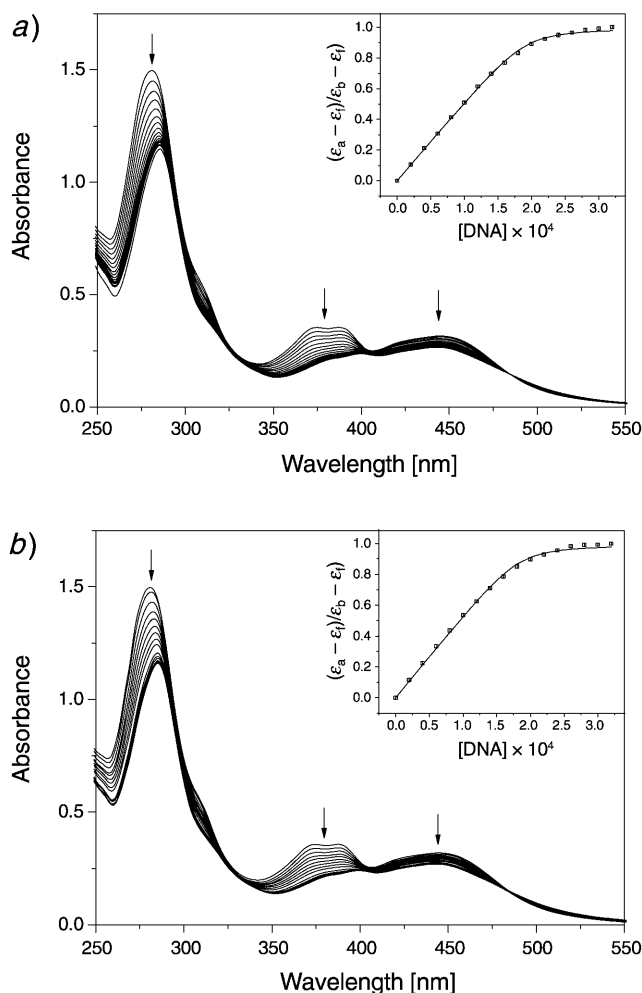


Fig. 4. Absorption spectra of a)  $\Delta$ - $[\text{Ru}(\text{bpy})_2(\text{dmppd})]^{2+}$  and b)  $\Lambda$ - $[\text{Ru}(\text{bpy})_2(\text{dmppd})]^{2+}$  in 5 mM *Tris*·*HCl* and 50 mM *NaCl* buffer (pH 7.0) at 25° in the presence of increasing amounts of *CT-DNA*.  $[\text{Ru}] = 20 \mu\text{M}$ ,  $[\text{DNA}] = 0\text{--}320 \mu\text{M}$  from top to bottom; arrows indicate the change in absorbance upon increasing the *DNA* concentration. Inset: plot of  $(\epsilon_a - \epsilon_f)/(\epsilon_b - \epsilon_f)$  vs.  $[\text{DNA}]$  for the titration of the  $\text{Ru}^{\text{II}}$  complexes.

mism reached 15.8 and 15.5% at a [DNA]/[Ru] ratio of 16.0 for  $\Delta$ - and  $\Lambda$ -[Ru(bpy)<sub>2</sub>(dmppd)]<sup>2+</sup>, respectively. The spectral characteristics suggest that there are some interactions between the ruthenium(II) complexes and DNA. To compare quantitatively the binding strength of  $\Delta$ - and  $\Lambda$ -[Ru(bpy)<sub>2</sub>(dmppd)]<sup>2+</sup>, their intrinsic binding constants  $K_b$  to DNA were obtained by monitoring the changes in absorbance at 444 nm with increasing concentration of DNA according to *Eqn. 1* [31]. In *Eqn. 1*, [DNA] is the concentration of DNA in base pairs and  $\varepsilon_a$  the apparent absorption coefficient;  $\varepsilon_f$  and  $\varepsilon_b$  correspond to  $A_{\text{obs}}/[\text{Ru}]$ , the extinction coefficient for the free ruthenium complex and the extinction coefficient for the ruthenium complex in the fully bound form, respectively.  $K_b$  is the equilibrium binding constant in M<sup>-1</sup>,  $C_t$  is the total metal complex concentration, and  $s$  is the binding size.

$$\frac{\varepsilon_a - \varepsilon_f}{\varepsilon_b - \varepsilon_f} = \frac{\sqrt{b - (b^2 - 2K_b^2 C_t [\text{DNA}]/s)}}{2K_b C_t} \quad (1a)$$

$$b = 1 + K_b C_t + K_b [\text{DNA}]/2s \quad (1b)$$

The intrinsic binding constants  $K_b$  of  $\Delta$ - and  $\Lambda$ -[Ru(bpy)<sub>2</sub>(dmppd)]<sup>2+</sup> were calculated to be  $(3.1 \pm 0.3) \cdot 10^5 \text{ M}^{-1}$  ( $s = 4.8 \pm 0.1$ ) and  $(2.8 \pm 0.3) \cdot 10^5 \text{ M}^{-1}$  ( $s = 4.6 \pm 0.1$ ), respectively. The values are smaller than those of [Ru(bpy)<sub>2</sub>(ppd)]<sup>2+</sup> ( $1.1 \cdot 10^6 \text{ M}^{-1}$ ) [14] and [Ru(bpy)<sub>2</sub>(dppz)]<sup>2+</sup> ( $> 10^6 \text{ M}^{-1}$ ) [11], which have a similar planarity and size, indicating that the presence of the bulky Me groups in dmppd might hinder severely the intercalation of  $\Delta$ - and  $\Lambda$ -[Ru(bpy)<sub>2</sub>(dmppd)]<sup>2+</sup> into DNA base pairs. The smaller binding constants of the latter complexes might also be due to the absence of H-bonds, which can operate in the case of [Ru(bpy)<sub>2</sub>(ppd)]<sup>2+</sup> between intercalated uracil groups and DNA base pairs resulting in a higher DNA affinity. On the other hand, the binding constants of  $\Delta$ - and  $\Lambda$ -[Ru(bpy)<sub>2</sub>(dmppd)]<sup>2+</sup> are greater than those of [Ru(bpy)<sub>2</sub>(dpq)]<sup>2+</sup> ( $5.9 \cdot 10^4 \text{ M}^{-1}$ ; dpq = dipyrido[3,2-*d*:2',3'-*f*]quinoxaline = pyrazino[1,2,3,4-*lmn*][1,10]phenanthroline) and [Ru(bpy)<sub>2</sub>(dpqc)]<sup>2+</sup> ( $8.5 \cdot 10^4 \text{ M}^{-1}$ ; dpqc = dipyrido-6,7,8,9-tetrahydrophenazine = 9a,10,11,12,13,13a-hexahydrodipyrido[3,2,1-*de*,1',2',3'-*mn*]phenazine) [18], suggesting that the coplanar area of the intercalating ligand is also a key factor operating on the interaction of complexes with DNA; a larger coplanar area may produce a higher DNA affinity.

The fact that the intrinsic binding constant of the  $\Delta$  enantiomer is stronger than that of the  $\Lambda$  enantiomers can be explained by a less deep intercalation of the  $\Lambda$  enantiomer than of the  $\Delta$  enantiomer, due to the steric matching of the bpy ligands with the right-handed helix of CT-DNA. The ratio of intrinsic binding constants of the  $\Delta$  and  $\Lambda$  enantiomers can serve as a quantitative parameter for the comparison of the enantioselectivity of different DNA intercalators. The value of  $K_b(\Delta)/K_b(\Lambda)$  of [Ru(bpy)<sub>2</sub>(dmppd)]<sup>2+</sup> is 1.1, which is comparable with those of reported ruthenium(II) complexes (from 1.1 to 1.5) [28][32]. The enantioselectivity of [Ru(bpy)<sub>2</sub>(dmppd)]<sup>2+</sup> is relatively small, most probably because the binding of dmppd to DNA base pairs is relatively strong, rendering the steric effect between the bpy ligands and the DNA helix less significant. A higher enantioselectivity may be expected in the complexes with a lower DNA affinity or by replacing the bpy ligands by other structurally special ligands.

2.3.2. *Competitive Binding Experiments.* In the absence of DNA, complex  $[\text{Ru}(\text{bpy})_2(\text{ppd})]^{2+}$  shows negligible luminescence in buffer. Upon addition of DNA, however, luminescence is increased, displaying the light-switch behaviors of  $[\text{Ru}(\text{bpy})_2(\text{ppd})]^{2+}$ . However, the complexes  $\Delta$ - and  $\Lambda$ - $[\text{Ru}(\text{bpy})_2(\text{dmppd})]^{2+}$ , emit a very weak luminance at 603 nm (exciting at 440 nm) in aqueous buffer in the absence of DNA. After binding with DNA, there were only small increases in the intensity of the emission band. This somewhat surprising finding may be understood by the assumption that the presence of two bulky Me groups in the intercalating ligand dmppd makes it difficult for  $\Delta$ - and  $\Lambda$ - $[\text{Ru}(\text{bpy})_2(\text{dmppd})]^{2+}$  to intercalate into DNA as deeply as  $[\text{Ru}(\text{bpy})_2(\text{ppd})]^{2+}$  does. Therefore, the N-atoms of the phenazine moiety are on the outside of the DNA base pairs and thus still accessible to the  $\text{H}_2\text{O}$  molecules of the buffer, which quench the luminance of the DNA-bound ruthenium(II) complexes *via* H-bonding and/or excited-state proton transfer [33–36].

For complexes exhibiting a weak emission intensity and a small enhancement in the presence of DNA, competitive binding to DNA of the complexes with ethidium bromide (EB = 3,8-diamino-5-ethyl-6-phenylphenanthridinium bromide) provides rich informations regarding the nature of DNA binding and the relative DNA-binding affinity [37][38]. EB emits intense fluorescence in the presence of DNA, due to its strong intercalation between the adjacent DNA base pairs of DNA ( $K_b = 1.4 \cdot 10^6 \text{ M}^{-1}$ ) [39]. If this enhanced fluorescence is reduced by addition of a second intercalative molecule, it will be an evidence of the intercalation of the second molecule. *Fig. 5* shows the changes in the emission spectra of EB-bound CT-DNA with increasing concentrations of  $\Delta$ - and  $\Lambda$ - $[\text{Ru}(\text{bpy})_2(\text{dmppd})]^{2+}$ . A clear decrease of the emission intensity was observed on the addition of the complexes to the EB-bound DNA solutions, indicating the intercalation of the complexes accompanied by the replacement of the EB molecules. Moreover,  $\Delta$ - $[\text{Ru}(\text{bpy})_2(\text{dmppd})]^{2+}$  reduced the luminance of DNA-bound EB to a greater extent than its  $\Lambda$  enantiomer at the same concentrations, implying that the  $\Delta$  enantiomer has a better DNA affinity than its  $\Lambda$  enantiomer.

2.3.3. *Viscosity Studies.* Optical photophysical probes generally provide necessary but not sufficient clues to support a binding mode. Viscosity measurements that are sensitive to the change of the length of the DNA are regarded as the least ambiguous and the most critical tests of binding mode in solution in the absence of crystallographic structural data [40–42]. To further elucidate the binding mode of the present complexes, viscosity measurements were carried out on CT-DNA by varying the concentration of the added complexes. A classical intercalation model demands that the DNA helix must lengthen as base pairs are separated to accommodate the binding ligand, leading to an increase of the viscosity of the DNA solution [43–45].

The effects of  $\Delta$ - and  $\Lambda$ - $[\text{Ru}(\text{bpy})_2(\text{dmppd})]^{2+}$ ,  $[\text{Ru}(\text{bpy})_3]^{2+}$ ,  $[\text{Ru}(\text{bpy})_2(\text{ppd})]^{2+}$ , and EB on the viscosity of rod-like DNA are shown in *Fig. 6*. EB increases the relative specific viscosity strongly by lengthening the DNA double helix through intercalation, while  $[\text{Ru}(\text{bpy})_3]^{2+}$ , which is known to bind with DNA in the electrostatic mode, exerts essentially no effect on DNA viscosity. On increasing the amounts of  $\Delta$ - and  $\Lambda$ - $[\text{Ru}(\text{bpy})_2(\text{dmppd})]^{2+}$ , the relative viscosity of DNA increased steadily, similarly to the behavior of EB and  $[\text{Ru}(\text{bpy})_2(\text{ppd})]^{2+}$ . The increased degree of viscosity, which may depend on the affinity to DNA, follow the order of  $\text{EB} > [\text{Ru}(\text{bpy})_2(\text{ppd})]^{2+} > \Delta$ - $[\text{Ru}(\text{bpy})_2(\text{dmppd})]^{2+} > \Lambda$ - $[\text{Ru}(\text{bpy})_2(\text{dmppd})]^{2+}$ . These results suggest that complex



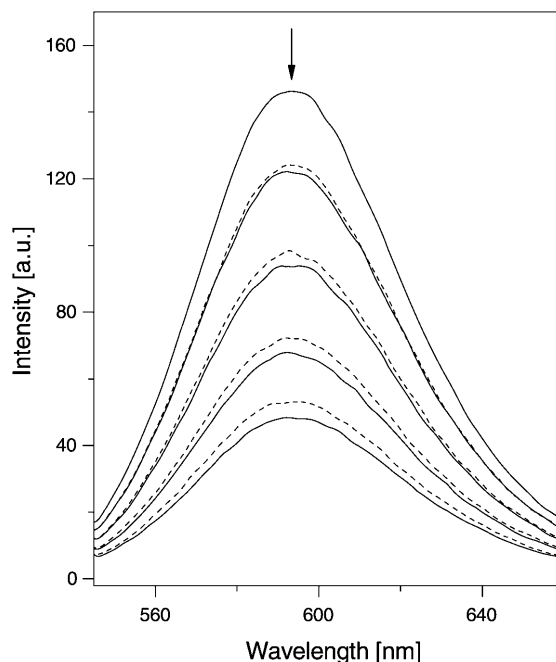


Fig. 5. Changes in the emission spectra of EB-bound CT-DNA in 5 mM Tris·HCl and 50 mM NaCl buffer (pH 7.0; [EB]=1.0  $\mu\text{M}$ , [DNA]=20.0  $\mu\text{M}$ ) with increasing concentrations of  $\Delta$ -[Ru(bpy)<sub>2</sub>(dmppd)]<sup>2+</sup> (—) and  $\Lambda$ -[Ru(bpy)<sub>2</sub>(dmppd)]<sup>2+</sup> (---) from 0 to 4.0  $\mu\text{M}$ . Arrow shows the intensity change upon increasing concentrations of the complex.

$\Delta$ -[Ru(bpy)<sub>2</sub>(dmppd)]<sup>2+</sup> and  $\Lambda$ -[Ru(bpy)<sub>2</sub>(dmppd)]<sup>2+</sup> intercalate between the base pairs of DNA, in accord with the spectroscopic results described above.

2.3.4. *Thermal Denaturation Study.* The thermal behavior of DNA in the presence of complexes can give insight into their conformational changes when temperature is raised, and offer information about the interaction strength of complexes with DNA. It is well known that when the temperature in the solution increases, the double-stranded DNA gradually dissociates to single strands, generating a hyperchromic effect in the absorption spectra of the DNA bases ( $\lambda_{\text{max}}$  260 nm). To identify this transition process, the melting temperature  $T_m$ , which is defined as the temperature where half of the total base pairs is unbonded, is usually determined. According to [46][47], the intercalation of metallointercalators generally results in a considerable increase of  $T_m$ . The melting curves of CT-DNA in the absence and presence of  $\Delta$ - and  $\Lambda$ -[Ru(bpy)<sub>2</sub>(dmppd)]<sup>2+</sup> are presented in Fig. 7. For CT-DNA in buffer B (*Exper. Part*), a  $T_m$  of  $61.7 \pm 0.2^\circ$  was determined. On addition of  $\Delta$ - or  $\Lambda$ -[Ru(bpy)<sub>2</sub>(dmppd)]<sup>2+</sup>, the  $T_m$  of the DNA increased to  $68.0 \pm 0.2^\circ$  and  $66.2 \pm 0.2^\circ$ , respectively, at a concentration ratio [DNA]/[Ru] of 10:1. The large increase (6.3 and  $4.5^\circ$ ) in  $T_m$  is comparable to that observed for classical intercalators [45–47].

The DNA intrinsic binding constant at  $T_m$  can be obtained from the *McGhee* equation (Eqn. 2), where  $T_m^0$  is the melting temperature of CT-DNA alone,  $T_m$  the melting temperature in the presence of the ruthenium(II) complex,  $\Delta H_m$  the enthalpy of DNA

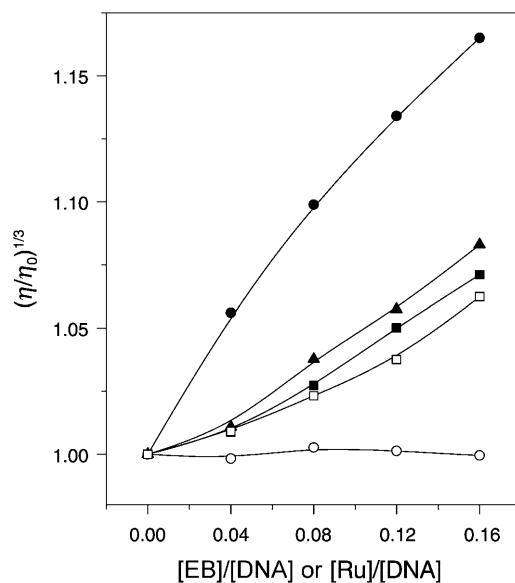


Fig. 6. Effect of increasing amounts of ethidium bromide ( $\bullet$ ),  $[Ru(bpy)_3]^{2+}$  ( $\circ$ ),  $[Ru(bpy)_2(ppd)]^{2+}$  ( $\blacktriangle$ ),  $\Delta$ - $[Ru(bpy)_2(dmppd)]^{2+}$  ( $\blacksquare$ ), and  $\Lambda$ - $[Ru(bpy)_2(dmppd)]^{2+}$  ( $\square$ ) on the relative viscosity of CT-DNA at  $28 (\pm 0.1)^\circ$ . Total concentration of DNA = 0.5 mM.

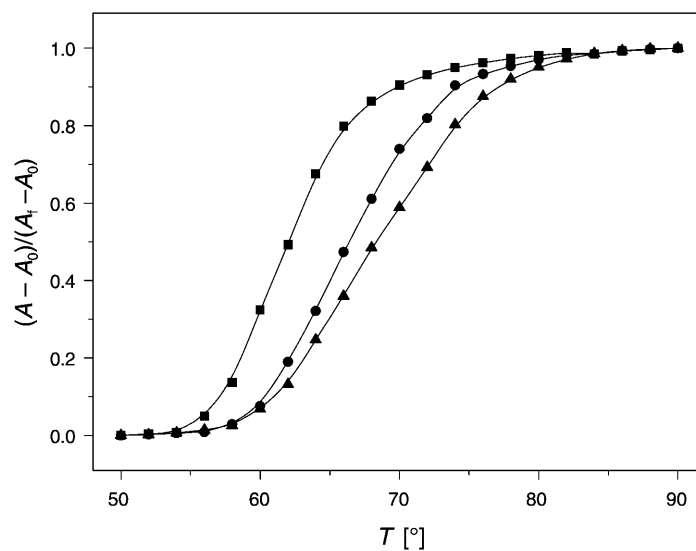


Fig. 7. Melting curves of CT-DNA ( $100 \mu\text{M}$ ) at  $260 \text{ nm}$  in the absence ( $\blacksquare$ ) and the presence of  $\Delta$ - $[Ru(bpy)_2(dmppd)]^{2+}$  ( $\blacktriangle$ ) and  $\Lambda$ - $[Ru(bpy)_2(dmppd)]^{2+}$  ( $\bullet$ ).  $[Ru^{II} \text{ complexes}] = 10 \mu\text{M}$ .

(per base pair),  $R$  the gas constant,  $K$  the DNA-binding constant at  $T_m$ ,  $L$  the free complex concentration (approximated at  $T_m$  by the total complex concentration), and  $n$  the size of the binding site.

$$\frac{1}{T_m^0} - \frac{1}{T_m} = \left( \frac{R}{\Delta H_m} \right) \ln(1 + KL)^{1/n} \quad (2)$$

For the CT-DNA used in these studies, under identical solution conditions, a melting enthalpy of  $6.9 \text{ kcal mol}^{-1}$  was determined by differential scanning calorimetry [41]. On the basis of the neighbor-exclusion principle, the values of  $n$  for complexes  $\Delta$ - and  $\Lambda$ -[Ru(bpy)<sub>2</sub>(dmppd)]<sup>2+</sup> were assumed to be 2.0 bp. By substitution of the required parameters into Eqn. 2,  $K$  was determined to be  $4.7 \cdot 10^4 \text{ M}^{-1}$  at  $68.0^\circ$  for  $\Delta$ -[Ru(bpy)<sub>2</sub>(dmppd)]<sup>2+</sup> and  $3.2 \cdot 10^4 \text{ M}^{-1}$  at  $66.2^\circ$  for  $\Lambda$ -[Ru(bpy)<sub>2</sub>(dmppd)]<sup>2+</sup>. The standard enthalpy, standard entropy, and standard free-energy change of the binding of  $\Delta$ - and  $\Lambda$ -[Ru(bpy)<sub>2</sub>(dmppd)]<sup>2+</sup> to CT-DNA were determined by *van't Hoff's* equations (Eqns. 3–5), where  $K_1$  and  $K_2$  are the DNA-binding constants of the metal complex at temperatures  $T_1$  and  $T_2$ , respectively, and  $\Delta H^0$ ,  $\Delta G^0$ , and  $\Delta S^0$  the standard enthalpy, standard free-energy, and standard entropy change of the metal-complex-binding to DNA, respectively. The values of  $\Delta H^0$ ,  $\Delta G^0$ , and  $\Delta S^0$  were found to be  $-37.1 \text{ kJ mol}^{-1}$ ,  $-31.3 \text{ kJ mol}^{-1}$ , and  $-19.5 \text{ J mol}^{-1} \text{ K}^{-1}$  for  $\Delta$ -[Ru(bpy)<sub>2</sub>(dmppd)]<sup>2+</sup>, and  $-35.3 \text{ kJ mol}^{-1}$ ,  $-31.1 \text{ kJ mol}^{-1}$ , and  $-14.1 \text{ J mol}^{-1} \text{ K}^{-1}$  for  $\Lambda$ -[Ru(bpy)<sub>2</sub>(dmppd)]<sup>2+</sup>, respectively. The negative  $\Delta G^0$  value suggests that the energy of the complex–DNA adduct is lower than the sum of the energies of the free complex and DNA. The negative  $\Delta H^0$  suggests that the binding of the complex to DNA at  $25^\circ$  is exothermic and driven by enthalpy. The negative entropy values indicate that the degree of freedom of the Ru<sup>II</sup> complexes is decreased after the binding, and that the DNA conformational freedom is also reduced upon complex–DNA binding.

$$\ln \left( \frac{K_1}{K_2} \right) = \frac{\Delta H^0}{R} \left( \frac{T_1 - T_2}{T_1 T_2} \right) \quad (3)$$

$$\Delta G^0 = -RT \ln K \quad (4)$$

$$\Delta G^0 = \Delta H^0 - T\Delta S^0 \quad (5)$$

**2.3.5. Circular-Dichroism (CD) Spectra.** CD Spectra have been utilized as a powerful tool for exploring the chiral aspect of compounds. Studying the enantioselective complex–DNA binding by CD may furnish direct informations on how the DNA helix and enantiomeric complexes interact and thus reveal the influence of each enantiomer of a given complex on the DNA-binding strength. Thus, the CD spectra of the free and fully DNA-bound  $\Delta$ - and  $\Lambda$ -[Ru(bpy)<sub>2</sub>(dmppd)]<sup>2+</sup> complexes in buffer A (*Exper. Part*) were compared (*Fig. 8, a*). In the excitation region, the CD spectrum of free  $\Delta$ -[Ru(bpy)<sub>2</sub>(dmppd)]<sup>2+</sup> is characterized by a negative band around 291 nm and that of  $\Lambda$ -[Ru(bpy)<sub>2</sub>(dmppd)]<sup>2+</sup> by a positive one. Upon addition of CT-DNA to saturation, the peak at 291 nm of  $\Delta$ - and  $\Lambda$ -[Ru(bpy)<sub>2</sub>(dmppd)]<sup>2+</sup> shifted to 290 nm with a moderate enhancement of 17 and 11%, respectively. This result may be due to the different matching between the enantiomers and DNA or to the different binding sites of the enantiomers, as DNA is a flexible double helix, and the complex can intercalate towards the DNA helix axis from any direction [28][32].

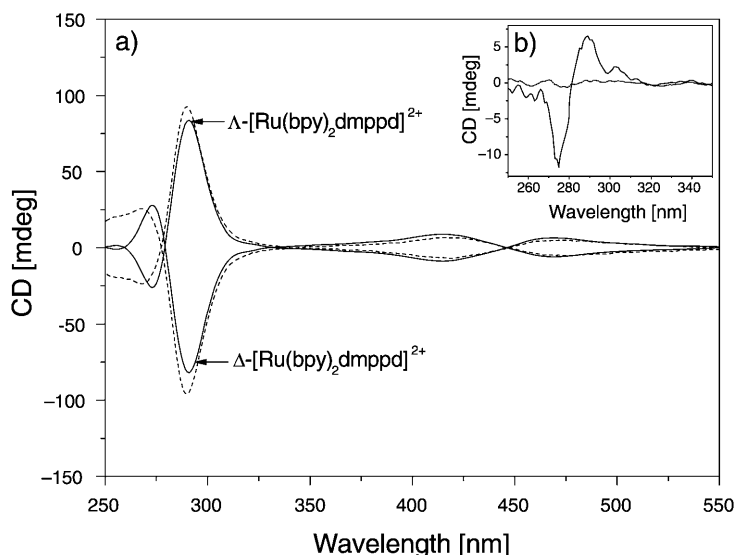


Fig. 8. a) CD Spectra of  $\Delta$ - $[\text{Ru}(\text{bpy})_2(\text{dmppd})]^{2+}$  and  $\Lambda$ - $[\text{Ru}(\text{bpy})_2(\text{dmppd})]^{2+}$  in 5 mM Tris-HCl and 50 mM NaCl (pH 7.0) in the absence (—) and presence of CT-DNA (---) ( $[\text{Ru}] = 20 \mu\text{M}$ ,  $[\text{DNA}] = 400 \mu\text{M}$ ). b) CD Spectra of the dialyzate obtained after 72 h of dialysis of 20 ml of racemic  $[\text{Ru}(\text{bpy})_2(\text{dmppd})]^{2+}$  (50  $\mu\text{M}$ ) against 10 ml of CT-DNA (1.0 mM) (the flat curve exhibiting CD [mdeg] ca. 0 is due to a dialyzate obtained similarly with  $[\text{Ru}(\text{bpy})_2(\text{ppd})]^{2+}$ ).

Equilibrium dialysis experiments may offer another opportunity to examine the enantioselectivity of complexes binding to DNA. The CD spectra in the UV region of the racemic solution of  $[\text{Ru}(\text{bpy})_2(\text{dmppd})]^{2+}$ , consisting of equivalent amounts of  $\Delta$ - and  $\Lambda$ - $[\text{Ru}(\text{bpy})_2(\text{dmppd})]^{2+}$ , and of  $[\text{Ru}(\text{bpy})_2(\text{ppd})]^{2+}$ , after dialysis against CT-DNA for 72 h, are shown in Fig. 8, b. For  $[\text{Ru}(\text{bpy})_2(\text{ppd})]^{2+}$ , because of its high DNA-binding ability, both  $\Delta$ - and  $\Lambda$ - $[\text{Ru}(\text{bpy})_2(\text{ppd})]^{2+}$  can intercalate into the DNA base pairs effectively, and no difference between the two enantiomers was observed. In the case of  $[\text{Ru}(\text{bpy})_2(\text{dmppd})]^{2+}$ , the introduction of the two Me groups decreased the DNA affinity of the complex, and the influence of the conformation of DNA and of the binding site or binding direction of the complex became more essential. Comparing the CD spectrum of the dialyzate (Fig. 8, b) with the CD spectra of free  $\Delta$ - and  $\Lambda$ - $[\text{Ru}(\text{bpy})_2(\text{dmppd})]^{2+}$  (Fig. 8, a) revealed that in the dialyzate more left-handed  $\Lambda$  enantiomer than right-handed  $\Delta$  enantiomer was left unbound. This can well be explained by a binding model involving a greater affinity of the right-handed propeller-like structure of the  $\Delta$  enantiomer to the right-handed CT-DNA helix, as compared to the  $\Lambda$  enantiomer, due to the appropriate steric matching [48].

**3. Conclusions.** – In summary, the two chiral ruthenium(II) complexes  $\Delta$ - and  $\Lambda$ - $[\text{Ru}(\text{bpy})_2(\text{dmppd})]^{2+}$  were synthesized and characterized. The results of spectroscopic titrations, competitive binding experiments, viscosity measurements, thermal DNA denaturation, and CD studies suggest that both complexes bind to DNA in an intercalative mode, and that the  $\Delta$  enantiomer has a greater DNA affinity than the  $\Lambda$  enan-

tiomer. The steric effect of the Me groups, the planarity of the intercalative ligand, and the energy and population of the MOs are probably the factors which reduce the DNA-binding ability of complexes. We hope that our results are of value in the further understanding of the efficiency and selectivity of DNA recognition by (polypyridine)ruthenium(II) complexes, as well as in laying the foundation for the rational design of new useful site-specific DNA probes and inorganic-complex nucleases.

We gratefully acknowledge support by the *National Natural Science Foundation of China*, the *Natural Science Foundation of Guangdong Province*, the *Research Fund for the Doctoral Program of Higher Education*, and the *State Key Laboratory of Coordination Chemistry* at Nanjing University.

### Experimental Part

*General.* All materials were commercially available and of their highest available purity. Calf-thymus DNA (CT-DNA) was obtained from *Sigma*. The dialysis membrane was purchased from *Union Carbide Co.* and treated by means of a general procedure before use [49]. The ligand dmppd was prepared and characterized according to [15].  $\Delta$ -[Ru(bpy)<sub>2</sub>(py)<sub>2</sub>][*O,O'*-dibenzoyl-*D*-tartrate]·12 H<sub>2</sub>O and  $\Lambda$ -[Ru(bpy)<sub>2</sub>(py)<sub>2</sub>][*O,O'*-dibenzoyl-*L*-tartrate]·12 H<sub>2</sub>O were prepared according to [16]; only the crystalline samples were used to assure the enantiomer purity. UV/VIS Spectra: *Perkin-Elmer-Lambda-850* spectrophotometer. Emission spectra: *Perkin-Elmer L55* spectrofluorophotometer. CD Spectra: *JASCO-J810* spectrometer;  $\lambda$  in nm,  $\Delta\epsilon$  in  $\text{m}^{-1}\text{cm}^{-1}$ . <sup>1</sup>H-NMR Spectra: *Varian-INOVA-500NB* superconducting FT spectrometer; (CD<sub>3</sub>)<sub>2</sub>SO as solvent at r.t. and SiMe<sub>4</sub> as internal standard;  $\delta$  in ppm, *J* in Hz. Electro spray (ES) MS: *LCQ* system (*Finnigan MAT*, USA); MeCN as mobile phase; spray voltage 4.50 KV, tube lens offset 30.00 V, capillary voltage 23.00 V, and capillary temp. 200°; *m/z* values for the major peaks in the isotope distribution. Microanalyses (C, H, and N): *Perkin-Elmer-240Q* elemental analyzer.

$\Delta$ -[10,12-Dimethylpteridino[6,7-*f*][1,10]phenanthroline-11,13(10H,12H)-dione- $\kappa\text{N}^4,\kappa\text{N}^5$ ]bis(2,2'-bipyridine- $\kappa\text{N}^1,\kappa\text{N}^{1'}$ )ruthenium(II) Diperchlorate Hydrate ( $\Delta$ -[Ru(bpy)<sub>2</sub>dmppd](ClO<sub>4</sub>)<sub>2</sub>·H<sub>2</sub>O). A mixture of  $\Delta$ -[Ru(bpy)<sub>2</sub>(py)<sub>2</sub>][*O,O'*-dibenzoyl-*D*-tartrate]·12 H<sub>2</sub>O (130 mg, 0.1 mmol), dmppd (69 mg, 0.2 mmol), ethylene glycol (9 ml), and H<sub>2</sub>O (1 ml) was refluxed for 8 h under Ar. The cooled mixture was diluted with H<sub>2</sub>O (30 ml) and filtered to remove the excess of ligand dmppd. Sat. aq. NaClO<sub>4</sub> soln. was added under vigorous stirring. The orange solid was collected, washed with small amounts of icy H<sub>2</sub>O, EtOH and Et<sub>2</sub>O, dried under vacuum, and purified by column chromatography (neutral alumina, MeCN). The red product was then recrystallized from Et<sub>2</sub>O/MeCN and then dried under vacuum for 10 h: 70 mg (72%). CD (H<sub>2</sub>O): 469 (−9.1), 416 (13.3), 291 (−124.1), 273 (42.1). <sup>1</sup>H-NMR ((CD<sub>3</sub>)<sub>2</sub>SO): 9.57 (*d*, *J* = 8.0, 1 H); 9.38 (*d*, *J* = 8.0, 1 H); 8.84 (*t*, 4 H); 8.26 (*d*, *J* = 8.0, 1 H); 8.22 (*d*, *J* = 8.0, 1 H); 8.20 (*t*, 2 H); 8.11 (*t*, 2 H); 8.00 (*t*, 2 H); 7.81 (*d*, *J* = 8.0, 2 H); 7.70 (*t*, 2 H); 7.58 (*t*, 2 H); 7.35 (*t*, 2 H); 3.84 (*s*, 3 H); 3.46 (*s*, 3 H). ES-MS (MeCN): 857.1 ([*M* − ClO<sub>4</sub>]<sup>+</sup>), 757.6 ([*M* − 2 ClO<sub>4</sub> − H]<sup>+</sup>), 378.8 ([*M* − 2 ClO<sub>4</sub>]<sup>2+</sup>). Anal. calc. for C<sub>38</sub>H<sub>28</sub>Cl<sub>2</sub>N<sub>10</sub>O<sub>10</sub>Ru·H<sub>2</sub>O: C 46.83, H 3.10, N 14.37; found: C 46.61, H 3.24, N 14.08.

$\Lambda$ -[10,12-Dimethylpteridino[6,7-*f*][1,10]phenanthroline-11,13(10H,12H)-dione- $\kappa\text{N}^4,\kappa\text{N}^5$ ]bis(2,2'-bipyridine- $\kappa\text{N}^1,\kappa\text{N}^{1'}$ )ruthenium(II) Diperchlorate Hydrate ( $\Lambda$ -[Ru(bpy)<sub>2</sub>dmppd](ClO<sub>4</sub>)<sub>2</sub>·H<sub>2</sub>O). This red complex was synthesized as described for  $\Delta$ -[Ru(bpy)<sub>2</sub>dmppd](ClO<sub>4</sub>)<sub>2</sub>·H<sub>2</sub>O, with  $\Lambda$ -[Ru(bpy)<sub>2</sub>(py)<sub>2</sub>][*O,O'*-dibenzoyl-*L*-tartrate]·12 H<sub>2</sub>O (130 mg, 0.1 mmol): 78 mg (80%). CD (H<sub>2</sub>O): 468 (9.8), 415 (−13.2), 291 (126.7), 273 (−39.4). <sup>1</sup>H-NMR ((CD<sub>3</sub>)<sub>2</sub>SO): 9.57 (*d*, *J* = 8.0, 1 H); 9.36 (*d*, *J* = 8.0, 1 H); 8.84 (*t*, 4 H); 8.27 (*d*, *J* = 8.0, 1 H); 8.22 (*d*, *J* = 8.0, 1 H); 8.20 (*t*, 2 H); 8.11 (*t*, 2 H); 8.01 (*t*, 2 H); 7.81 (*d*, *J* = 8.0, 2 H); 7.71 (*t*, 2 H); 7.58 (*t*, 2 H); 7.35 (*t*, 2 H); 3.84 (*s*, 3 H); 3.46 (*s*, 3 H). ES-MS (MeCN): 857.1 ([*M* − ClO<sub>4</sub>]<sup>+</sup>), 757.6 ([*M* − 2 ClO<sub>4</sub> − H]<sup>+</sup>), 378.8 ([*M* − 2 ClO<sub>4</sub>]<sup>2+</sup>). Anal. calc. for C<sub>38</sub>H<sub>28</sub>Cl<sub>2</sub>N<sub>10</sub>O<sub>10</sub>Ru·H<sub>2</sub>O: C 46.83, H 3.10, N 14.37; found: C 46.57, H 3.28, N 14.12.

*DNA-Binding Experiments.* The DNA-binding experiments were performed at 25.0 ± 0.2°. Buffer *A* (5 mM *Tris*·HCl, 50 mM NaCl, pH 7.0, *Tris* = tris(hydroxymethyl)aminomethane = 2-amino-2-(hydroxymethyl)propane-1,3-diol) was used for UV/VIS absorption titrations, competitive binding experiments,

viscosity measurements, and dialysis experiments. Buffer *B* (1.5 mM Na<sub>2</sub>HPO<sub>4</sub>, 0.5 mM NaH<sub>2</sub>PO<sub>4</sub>, 0.25 mM Na<sub>2</sub>H<sub>2</sub>edta (H<sub>4</sub>edta = ethylenediaminetetraacetic acid = *N,N'*-ethane-1,2-diylbis[*N*-(carboxymethyl)glycine]), pH 7.0) was used for thermal denaturation experiments. A soln. of CT-DNA gave a ratio of UV absorbance at 260 and 280 nm of 1.9:1, indicating that the DNA was sufficiently free of protein [50]. The DNA concentration per nucleotide was determined by absorption spectroscopy by using the molar absorption coefficient (6600 M<sup>-1</sup>cm<sup>-1</sup>) at 260 nm [51]. DNA stock solns. were stored at 4° and used within 4 days.

The UV/VIS absorption titrations of Ru<sup>II</sup> complexes in buffer *A* at 25° were performed by using a fixed complex concentration (20 μM), to which increments of the DNA stock soln. were added to a ratio [DNA]/[Ru] 16:1. Complex–DNA solns. were allowed to incubate for 5 min. before the UV/VIS spectra were recorded.

Thermal DNA-denaturation experiments were carried out with a spectrophotometer equipped with a *Peltier* temp.-controlling programmer (±0.1°). The temp. of the soln. was increased from 50 to 90° at a rate of 1°/min, and the absorbance at 260 nm was continuously monitored for solns. of CT-DNA (100 μM) in the absence and presence of the Ru<sup>II</sup> complex (10 μM). Data were presented as  $(A - A_0)/(A_f - A_0)$  vs. temp., where *A<sub>f</sub>*, *A<sub>0</sub>*, and *A* are the final, initial, and observed absorbance at 260 nm, resp.

Viscosity measurements were carried out with an *Ubbelohde* viscometer maintained at a constant temp. of 28.0 ± 0.1° in a thermostatic bath. DNA Samples of ca. 200 base pairs in average length were prepared by sonication to minimize complexities arising from DNA flexibility [52]. Flow time was measured with a digital stopwatch, and each sample was measured three times, and an average flow time was calculated. Data were presented as  $(\eta/\eta_0)^{1/3}$  vs. binding ratio [53], where  $\eta$  is the viscosity of DNA in the presence of complex and  $\eta_0$  is the viscosity of DNA alone.

CD Spectra of the complexes (20 μM) in the absence and presence of DNA (400 μM) were recorded in buffer *A* at r.t. Equilibrium dialyses were conducted at r.t. with 10 ml of CT-DNA (1.0 mM) scaled in a dialysis bag and 20 ml of the complex (50 μM) outside the bag with the soln. being stirred for 72 h; the CD spectra of the dialyzates outside the bag were recorded.

*Theoretical Calculations.* The DFT calculations were carried out with the Gaussian98 quantum chemistry program package [54] by using *Becke's* three-parameter hybrid functional (B3LYP) method [55] and LanL2DZ basis set (a double-zeta basis set containing effective core potential) [56]. The full geometry-optimization computations were carried out for the ground states (singlet state) of these complexes [57]. The stability of the optimized conformation of the complexes was confirmed by the frequency analysis, which shows no imaginary frequency for each energy minimum. To vividly depict the detail of the frontier MOs of complexes, the stereographs of some related MOs were visualized with the Molden v3.7 program based on the computational results.

## REFERENCES

- [1] 'DNA and RNA Binders: From Small Molecules to Drugs', Eds. M. Demeunynck, C. Bailly, and W. D. Wilson, Wiley-VCH, Weinheim, 2003.
- [2] 'Metallotherapeutic Drugs and Metal-Based Diagnostic Agents: The Use of Metals in Medicine', Eds. M. Gielen, E. R. T. Tiekink, John Wiley & Sons, Ltd., Chichester, UK, 2005.
- [3] 'Metal Ions in Biological Systems, Vol. 33', Eds. A. Sigel, and H. Sigel, Marcel Dekker, New York, 1996.
- [4] K. E. Erkkila, D. T. Odom, J. K. Barton, *Chem. Rev.* **1999**, *99*, 2777.
- [5] C. Metcalfe, J. A. Thomas, *Chem. Soc. Rev.* **2003**, *32*, 215.
- [6] L. N. Ji, X. H. Zou, J. G. Liu, *Coord. Chem. Rev.* **2001**, *216–217*, 513.
- [7] H. Chao, L. N. Ji, *Bioinorg. Chem. Appl.* **2005**, *3*, 15.
- [8] J. P. Rehmann, J. K. Barton, *Biochemistry* **1990**, *29*, 1701.
- [9] S. Satyanarayana, J. C. Dabrowiak, J. B. Chaires, *Biochemistry* **1992**, *31*, 9319.
- [10] L. M. Wilhelmsson, F. Westerlund, P. Lincoln, B. Nordén, *J. Am. Chem. Soc.* **2002**, *124*, 12092.
- [11] A. E. Friedman, J. C. Chambron, J. P. Sauvage, N. J. Turro, J. K. Barton, *J. Am. Chem. Soc.* **1990**, *112*, 4960.
- [12] A. E. Friedman, C. V. Kumar, N. J. Turro, J. K. Barton, *Nucleic Acids Res.* **1991**, *19*, 2595.

- [13] R. M. Hartshorn, J. K. Barton, *J. Am. Chem. Soc.* **1992**, *114*, 5919.
- [14] F. Gao, H. Chao, F. Zhou, Y. X. Yuan, B. Peng, L. N. Ji, *J. Inorg. Biochem.* **2006**, *100*, 1487.
- [15] K. J. Black, H. Huang, S. High, L. Starks, M. Olson, M. E. McGuire, *Inorg. Chem.* **1993**, *32*, 5591.
- [16] X. Hua, A. von Zelewsky, *Inorg. Chem.* **1995**, *34*, 5791; O. Morgan, S. Wang, S. A. Bae, R. J. Morgan, A. D. Baker, T. C. Streckas, R. Engel, *J. Chem. Soc., Dalton Trans.* **1997**, 3773; B. Kolp, H. Viebrock, A. von Zelewsky, D. Abeln, *Inorg. Chem.* **2001**, *40*, 1196.
- [17] C. Moucheron, A. Kirsch-De Mesmaeker, S. Choua, *Inorg. Chem.* **1997**, *36*, 584.
- [18] E. J. C. Olson, D. Hu, A. Hormann, A. M. Jonkman, M. R. Arkin, E. D. A. Stemp, J. K. Barton, P. F. Barbara, *J. Am. Chem. Soc.* **1997**, *119*, 11458.
- [19] S. Arounaguirri, B. G. Maiya, *Inorg. Chem.* **1999**, *38*, 842.
- [20] Q. X. Zhen, B. H. Ye, Q. L. Zhang, J. G. Liu, H. Li, L. N. Ji, L. Wang, *J. Inorg. Biochem.* **1999**, *76*, 47.
- [21] Q. X. Zhen, Q. L. Zhang, J. G. Liu, B. H. Ye, L. N. Ji, L. Wang, *J. Inorg. Biochem.* **2000**, *78*, 293.
- [22] H. Chao, W. J. Mei, Q. W. Huang, L. N. Ji, *J. Inorg. Biochem.* **2002**, *92*, 165.
- [23] H. Deng, H. Xu, Y. Yang, H. Li, H. Zou, L. H. Qu, L. N. Ji, *J. Inorg. Biochem.* **2003**, *97*, 207.
- [24] X. Hua, A. von Zelewsky, *Inorg. Chem.* **1995**, *34*, 5791.
- [25] R. Caspar, L. Musatkina, A. Tatosyan, H. Amouri, M. Gruselle, C. Guyard-Duhayon, R. Duval, C. Cordier, *Inorg. Chem.* **2004**, *43*, 7986.
- [26] J. K. Barton, J. S. Nowick, *J. Chem. Soc., Chem. Commun.* **1984**, 1650.
- [27] C. Hiort, P. Lincoln, B. Norden, *J. Am. Chem. Soc.* **1993**, *115*, 3448.
- [28] S. Shi, J. Liu, J. Li, K. C. Zheng, X. M. Huang, C. P. Tan, L. M. Chen, L. N. Ji, *J. Inorg. Biochem.* **2006**, *100*, 385.
- [29] K. Fukui, T. Yonezawa, H. Shingu, *J. Chem. Phys.* **1952**, *20*, 722.
- [30] G. Klopman, *J. Am. Chem. Soc.* **1968**, *90*, 223.
- [31] S. A. Lesko, R. J. Lorentzen, P. O. Ts'o, *Biochemistry* **1980**, *19*, 3023.
- [32] W. J. Mei, J. Liu, K. C. Zheng, L. J. Lin, H. Chao, A. X. Li, F. C. Yun, L. N. Ji, *Dalton Trans.* **2003**, *7*, 1352.
- [33] Y. Jenkins, A. E. Friedman, N. J. Turro, J. K. Barton, *Biochemistry* **1992**, *31*, 10809.
- [34] C. M. Dupureur, J. K. Barton, *J. Am. Chem. Soc.* **1994**, *116*, 10286.
- [35] C. Turro, S. H. Bossmann, Y. Jenkins, J. K. Barton, N. J. Turro, *J. Am. Chem. Soc.* **1995**, *117*, 9026.
- [36] R. B. Nair, B. M. Cullum, C. J. Murphy, *Inorg. Chem.* **1997**, *36*, 962.
- [37] B. C. Baguley, M. Lebret, *Biochemistry* **1984**, *23*, 937.
- [38] J. R. Lakowicz, G. Webber, *Biochemistry* **1973**, *12*, 4161.
- [39] J. B. Lepecep, C. Paoletti, *J. Mol. Biol.* **1967**, *27*, 87.
- [40] S. Satyanarsyana, J. C. Dabroniak, J. B. Chaires, *Biochemistry* **1992**, *31*, 9319.
- [41] S. Satyanarsyana, J. C. Dabroniak, J. B. Chaires, *Biochemistry* **1993**, *32*, 2573.
- [42] X. L. Hong, H. Chao, L. J. Lin, K. C. Zheng, H. Li, X. L. Wang, F. C. Yun, L. N. Ji, *Helv. Chim. Acta* **2004**, *87*, 1180.
- [43] R. B. Nair, B. M. Cullum, C. J. Murphy, *Inorg. Chem.* **1997**, *36*, 962.
- [44] B. C. Baguley, M. Lebret, *Biochemistry* **1984**, *23*, 937.
- [45] Y. J. Liu, H. Chao, J. H. Yao, H. Li, Y. X. Yuan, L. N. Ji, *Helv. Chim. Acta* **2004**, *87*, 3119.
- [46] M. J. Waring, *J. Mol. Biol.* **1965**, *13*, 269.
- [47] G. A. Neyhart, N. Grover, S. R. Smith, W. A. Kalsbeck, T. A. Fairly, M. Cory, H. H. Thorp, *J. Am. Chem. Soc.* **1993**, *115*, 4423.
- [48] J. K. Barton, *Science (Washington, D.C.)* **1986**, *233*, 727.
- [49] J. K. Barton, J. J. Dannenberg, A. L. Raphael, *J. Am. Chem. Soc.* **1984**, *106*, 2172.
- [50] J. Marmur, *J. Mol. Biol.* **1961**, *3*, 208.
- [51] M. E. Reichmann, S. A. Rice, C. A. Thomas, P. Doty, *J. Am. Chem. Soc.* **1954**, *76*, 3047.
- [52] J. B. Chaires, N. Dattagupta, D. M. Crothers, *Biochemistry* **1982**, *21*, 3933.
- [53] G. Cohen, H. Eisenberg, *Biopolymers* **1969**, *8*, 45.
- [54] M. J. Frisch, G. W. Trucks, H. B. Schlegel, G. E. Scuseria, M. A. Robb, J. R. Cheeseman, V. G. Zakrzewski, J. A. Montgomery Jr., R. E. Stratmann, J. C. Burant, S. Dapprich, J. M. Millam, A. D. Daniels, K. N. Kudin, M. C. Strain, O. Farkas, J. Tomasi, V. Barone, M. Cossi, R. Cammi, B. Mennucci, C. Pomelli, C. Adamo, S. Clifford, J. Ochterski, G. A. Petersson, P. Y. Ayala, Q. Cui, K. Morokuma, N.

- Rega, P. Salvador, J. J. Dannenberg, D. K. Malick, A. D. Rabuck, K. Raghavachari, J. B. Foresman, J. Cioslowski, J. V. Ortiz, A. G. Baboul, B. B. Stefanov, G. Liu, A. Liashenko, P. Piskorz, I. Komaromi, R. Gomperts, R. L. Martin, D. J. Fox, T. Keith, M. A. Al-Laham, C. Y. Peng, A. Nanayakkara, M. Challacombe, P. M. W. Gill, B. Johnson, W. Chen, M. W. Wong, J. L. Andres, C. Gonzalez, M. Head-Gordon, E. S. Replogle, J. A. Pople, 'Gaussian 98, Revision A.11.4', Gaussian, Inc., Pittsburgh PA, 2002.
- [55] A. D. Becke, *J. Chem. Phys.* **1993**, *98*, 1372; A. Görling, *Phys. Rev. A* **1996**, *54*, 3912; P. Hohenberg, W. Kohn, *Phys. Rev. B* **1964**, *136*, 864.
- [56] J. B. Foresman, Æ. Frisch, 'Exploring Chemistry with Electronic Structure Methods', 2nd edn., Gaussian Inc., Pittsburgh, PA, 1996; P. J. Hay, W. R. Wadt, *J. Chem. Phys.* **1985**, *82*, 270; W. R. Wadt, P. J. Hay, *J. Chem. Phys.* **1985**, *82*, 284.
- [57] A. Juris, V. Balzani, F. Barigelletti, S. Campagna, P. Belser, A. von Zelewsky, *Coord. Chem. Rev.* **1988**, *84*, 85.

Received May 17, 2006